Calcium channel subtypes in cat chromaffin cells

Almudena Albillos, Antonio R. Artalejo, Manuela G. López, Luis Gandía, Antonio G. García and Emilio Carbone*

*Departamento de Farmacología, Facultad de Medicina, Universidad Autónoma de Madrid, Avenida de Arzobispo Morcillo 4, 28029 Madrid, Spain and *Dipartimento di Anatomia e Fisiologia Umana, Corso Raffaello 30, 10125 Torino, Italy*

1. Using the patch-clamp technique we have investigated the kinetic and pharmacological properties of high-voltage-activated (HVA) Ca^{2+} channels in short-term-cultured cat chromaffin cells.

2. In 10 mM Ba^{2+}, HVA currents activated around -40 mV, reached maximal amplitude at 0 mV and reversed at about $+60$ mV. At 0 mV, HVA current activation was fast (mean τ_{act}, 2·45 ms), and followed by either an incomplete inactivation or by a second slow phase of activation (mean τ_{slow}, 36·8 ms) that was lost when Ba^{2+} was replaced by Ca^{2+}. HVA Ba^{2+} currents deactivate quickly on repolarization to -50 mV (mean τ_{deact}, 0·36 ms).

3. In most cells, HVA currents were sensitive to common dihydropyridine (DHP) derivatives. Nisoldipine blocked the currents maximally at low membrane potentials (mean block 76 % at -30 mV, 3 μM) and gradually less at higher voltages. Nisoldipine block was clearly time dependent (33 and 56 % after 30 and 600 ms, respectively, to 0 mV).

4. Bay K 8644 (3 μM) action was variable and caused (1) a 2- to 4-fold increase of Ba^{2+} currents at -40 to -20 mV, (2) a -15 mV shift of the current–voltage relationship and (3) a 10- to 20-fold prolongation of HVA channel deactivation at -50 mV.

5. Nisoldipine block and Bay K 8644 potentiation of HVA currents increased markedly in ω-conotoxin GVIA (ω-CgTX)-pretreated cells, suggesting an increased fraction of DHP-sensitive currents in these cells. Nisoldipine block of residual ω-CgTX-resistant currents was almost complete (mean block, 82 %) during pulses of 1 s to 0 mV.

6. The degree of inhibition produced by ω-CgTX (2 μM for 1 min) varied from cell to cell (mean block, 46 %) and was partly reversible. Residual ω-CgTX-resistant currents exhibited faster activation–deactivation kinetics than control currents.

7. The slow phase of HVA current activation was abolished if a conditioning prepulse of 40 ms to $+70$ mV preceded a test pulse to 0 mV. Double-pulse protocols caused an average current increase (facilitation) of 37 % that was voltage dependent and which correlated with the slow phase of Ca^{2+} channel activation. Facilitation was lost in most ω-CgTX-treated cells and was little affected by nisoldipine (3 μM) and Bay K 8644 (1 μM). Facilitation was potentiated in cells dialysed with 100 μM guanosine 5'-O-(3-thiotriphosphate) (GTP-γ-S) and fully prevented by 1 mM guanosine 5'-O-(2-thiodiphosphate) (GDP-β-S).

8. Our data suggest that in cat chromaffin cells, HVA currents and their 'facilitation' by conditioning prepulses are mostly due to DHP- and ω-CgTX-sensitive Ca^{2+} channels.

There is a wide consensus for the idea that the regulation of catecholamine release from cat adrenal glands is dominated by high-threshold L-type Ca^{2+} channels. Convincing evidence for this comes from experiments involving K^{+}-evoked secretory responses in perfused cat adrenal glands that appear to be highly sensitive to 1,4-dihydropyridine (DHP) Ca^{2+} channel blockers and activators (for a review see Artalejo, López, Castillo, Moro & García, 1988). In contrast to the feline response, the bovine adrenal secretory response is partly preserved in the

presence of DHPs (Gandía, Michelena, De Pascual, López & García, 1990). This could be due to the co-existence of mixed populations of DHP-resistant and DHP-sensitive Ca^{2+} channels in bovine chromaffin cells, as demonstrated recently by whole-cell (Hans, Illes & Takeda, 1990; Artalejo, Dahmer, Perlman & Fox, 1991a; Bossu, De Waard & Feltz, 1991a) and single Ca^{2+} channel current measurements (Artalejo, Mogul, Perlman & Fox, 1991b; Bossu, De Waard & Feltz, 1991b).

In view of these results, the question arises as to whether other high-voltage-activated (HVA) Ca^{2+} channels, besides L-type (DHP sensitive), are also expressed in cat chromaffin cells. If so, a second question then emerges concerning the possible role of these DHP-resistant Ca^{2+} channels, given that the cat adrenal K^{+}-secretion response is fully blocked by DHPs. In this paper we present a patch-clamp study which shows that whole-cell Ca^{2+} currents of cultured cat chromaffin cells are of two main types, namely the DHP-sensitive L-type and the ω-conotoxin (ω-CgTX)-sensitive N-type. As in bovine cells (Fenwick, Marty & Neher, 1982), Ca^{2+} currents in cat chromaffin cells can be facilitated by strong positive prepulses but, unlike the bovine situation (Artalejo et al. 1991a), facilitation is largely prevented by ω-CgTX and only weakly affected by DHPs. With respect to previously reported data in bovine chromaffin cells (Ceña, Stutzin & Rojas, 1989; Bossu et al. 1991a), HVA Ca^{2+} currents in cat chromaffin cells also exhibit significant differences in their kinetics and pharmacology.

METHODS

Isolation and culture of cat adrenal medulla chromaffin cells

Cats of both sexes, weighing 2·5–4 kg, were anaesthetized by I.P. administration of sodium pentobarbitone (50 mg kg^{-1}). A thin polyethylene cannula was inserted into the adrenal vein and both glands were removed. The cortex was pierced with an insulin needle to allow the exit of the perfusion fluid. First, glands were injected gently through the cannula with 5 ml of Ca^{2+}- and Mg^{2+}-free Locke solution of the following composition (mM): 154 NaCl, 3·6 KCl, 5·6 NaHCO$_3$, 5·6 glucose, and 10 Hepes buffer (pH 7·2) at room temperature. This wash-out procedure was repeated three times. Digestion of the medullae was achieved by injecting the glands twice, by means of a syringe, with 2·5 ml of a Ca^{2+}- and Mg^{2+}-free Locke solution containing 0·2 % w/v collagenase and 0·5 % w/v bovine serum albumin at 10 min intervals and at a temperature of 37 °C. This procedure was repeated three times. Following this, the glands were cut longitudinally and the liquified medullae were gently scraped out from the cortex. The collagenase was washed out of the cells with large volumes of Ca^{2+}- and Mg^{2+}-free Locke solution. After two washes, the cells were resuspended in Dulbecco's modified Eagle's medium (DMEM) supplemented with 5 % v/v fetal calf serum containing 50 i.u. ml^{-1} penicillin and 50 μg ml^{-1} streptomycin. Cells were plated on circular glass coverslips and incubated at 37 °C in a water-saturated, 5 % CO$_2$ atmosphere; they were

used within 1–5 days of plating. DMEM was replaced every 2 days by fresh medium.

Solutions

The external bath solution contained (mM): 155 NaCl, 10 BaCl$_2$ (or, when indicated, 10 CaCl$_2$), 1 MgCl$_2$, 10 Hepes (adjusted to pH 7·3 with NaOH, and 5 μM tetrodotoxin (TTX). These external solutions are referred to as 10 mM Ba^{2+} or 10 mM Ca^{2+}. The patch pipette solution contained (mM): 110 CsCl, 30 tetraethylammonium chloride (TEA), 2 MgCl$_2$, 10 EGTA, 3 glucose, 10 Hepes, 5 MgATP and 0·3 GTP (adjusted to pH 7·3 with NaOH).

Stock solutions (10 mM) of Bay K 8644 (1,4-dihydro-2,6-dimethyl-3-nitro-4-(2-trifluoromethylphenyl)-pyridine-5-carboxylic acid methyl ester) and nisoldipine (both kindly provided by Bayer AG, FRG) were prepared in ethanol and diluted in the external solution to the required final concentration (1–10 μM). ω-Conotoxin (ω-CgTX, fraction GVIA, Sigma, St Louis, MO, USA) was prepared as a 1 mM stock solution in distilled water and kept in aliquots at −20 °C until use. To maximize the block potency of ω-CgTX, some cells were chronically treated and exposed to the toxin (0·1–2 μM) for 4 h in DMEM at 37 °C. NaGTP, LiGTP-γ-S, LiGDP-β-S and MgATP were from Sigma.

External solutions were exchanged by fast superfusion using a modified, multibarrelled ejection, glass pipette (Carbone & Lux, 1987). The pipette had an opening of 50–100 μm and was positioned 50–100 μm away from the cell, which was superfused continuously throughout the whole experiment. Changes between control and test solutions were made manually through three stopcock valves. The flow rate was low (1–2 ml min^{-1}) and regulated by gravity to achieve complete replacement of the cell surroundings within 0·4–1 s.

Current measurements and analysis

Membrane currents were measured using the patch-clamp technique in the whole-cell configuration (Hamill, Marty, Neher, Sakmann & Sigworth, 1981). A List EPC-7 patch-clamp amplifier (List Electronics, Darmstadt, FRG) and pipettes of thin borosilicate glass with resistances of 2–4 MΩ, when filled with the standard Cs–TEA intracellular solution, were used. Current recordings were filtered at 3–10 kHz (−3 dB, 8-pole Bessel filter) and digitized at sampling intervals of 10–300 μs using a 12 bit A/D Tecmar LabMaster board (125 kHz) interfaced with an IBM computer. Stimulation and acquisition were made using pCLAMP software (Axon Instruments, Foster City, CA, USA). Off-line data analysis and curve fittings were made using AutesP programs (Garching Instruments, Munich, FRG) (Pollo, Lovallo, Sher & Carbone, 1992).

At rest, cells were clamped at −70 mV holding potential (V_h). Unless otherwise indicated, step depolarizations from V_h usually lasted 30–200 ms and were applied at intervals of 10–15 s to minimize the 'run-down' of Ca^{2+} channels (Fenwick et al. 1982). Ca^{2+} channel run-down was effectively reduced, but not eliminated, by adding MgATP (5 mM) to the pipette solution. In some experiments, longer depolarizing pulses (0·6–1 s) were applied. Capacitive transients and leakage currents were minimized by a preliminary electronic compensation and by subtracting Cd^{2+}-insensitive currents off-line (Carbone, Sher & Clementi, 1990). Membrane currents were always fully blocked by 200 μM Cd^{2+}, suggesting the absence of K^{+} and Cl^{-} currents in our recordings. The presence of K^{+} currents was further prevented by using K^{+}-free extracellular

media. Data are expressed as means ± S.E.M. for n number of cells.

Filtering, capacitive transients and series resistance compensation were particularly critical when measuring tail currents. Cells were spherical and had a diameter of 10–15 μm; their total capacitance was between 10 and 20 pF. The electrode series resistance (2·8–6·0 MΩ), after breaking into the cell, was estimated by means of the potentiometer setting and compensated by about 60 % to give a fast-clamp response of 20–35 μs. The compensation setting for the test pulse was checked and readjusted after each sequence of pulse protocols was terminated. Tail currents were filtered at 10 kHz and sampled at intervals of 10 μs. Experiments were performed at room temperature (22–24 °C).

RESULTS

Kinetics and permeability of HVA Ca²⁺ channels in cat chromaffin cells

Ca²⁺ currents in cat chromaffin cells, recorded in 10 mM external Ca²⁺ concentration ($[Ca^{2+}]_o$), were shown to activate around −30 mV, to reach maximal amplitude at about +10 mV and to revert near +60 mV (Fig. 1A and C, open circles). The current size varied greatly from cell to cell. Freshly dissociated cells were easier to patch, but usually had smaller current amplitudes than cells which had been cultured for 3 days (peak I_{Ca}, 75 ± 12 pA; $n = 16$). In more than 200 cells we also found no sign of fast-inactivating, low-voltage-activated (LVA, T-type) Ca²⁺ currents even using very negative holding potentials (−90 mV) that favour their reprime from resting inactivation (Carbone & Lux, 1987). Thus, Ca²⁺ currents in cat chromaffin cells appeared to flow almost exclusively through high-voltage-activated (HVA) Ca²⁺ channels.

The time constant of activation (τ_{act}) of HVA Ca²⁺ currents increased from 1·4 ms at −20 mV to 2·3 ms at 0 mV and decreased again to a minimum of 0·6 ms at +40 mV, giving a bell-shaped $\tau_{act}(V)$ curve that peaked at around 0 mV, as described for other voltage-dependent Ca²⁺ channel conductances (open circles in Fig. 2A). Below

Figure 1. Activation and inactivation kinetics of HVA Ca²⁺ and Ba²⁺ currents in a cat chromaffin cell
In A and B the overlapped current traces were recorded on step depolarizations from −40 to +60 mV with step increments of 20 mV. Holding potential (V_h) was −70 mV. C, I–V plots of the amplitude of Ba²⁺ (●) and Ca²⁺ currents (○) *versus* voltage. The size of the current varied substantially from cell to cell. They were normalized with respect to the maximum value of Ba²⁺ currents at 0 mV and plotted as means ± S.E.M. for $n = 11$ cells (Ba²⁺) and $n = 5$ cells (Ca²⁺). Notice the slight shift towards positive voltages of the negative slope region and maximal current when Ba²⁺ was replaced by Ca²⁺ in the bath.
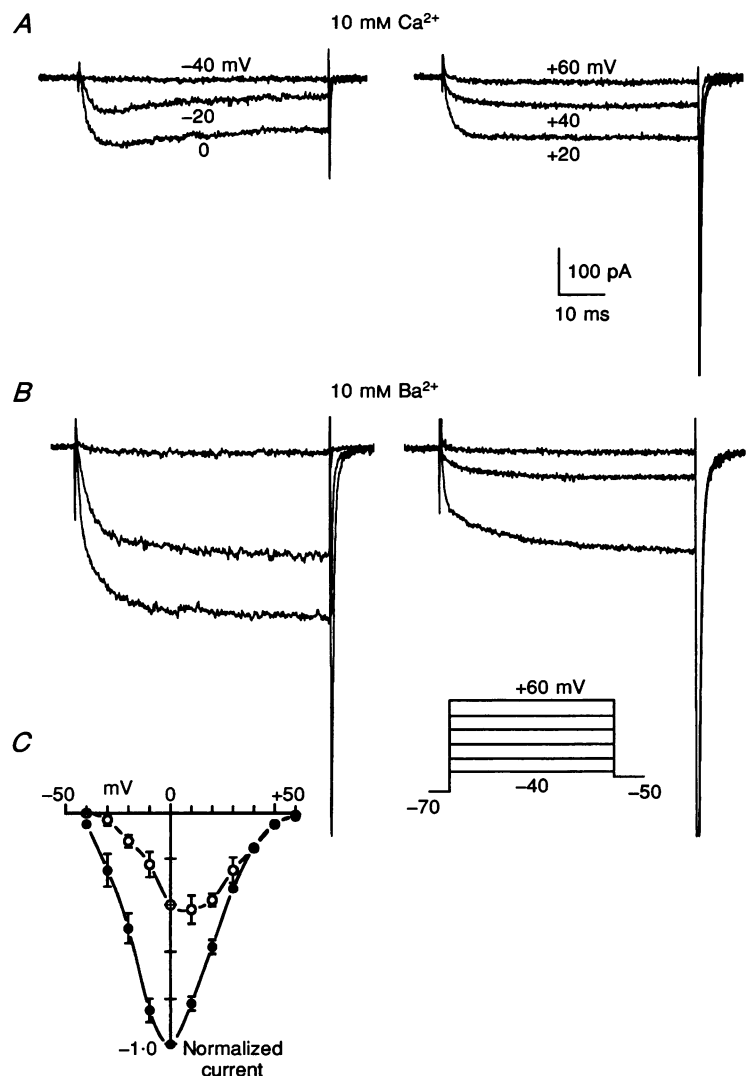
0 mV, HVA Ca^{2+} currents exhibited the usual sign of time-dependent inactivation that was faster soon after the peak current than at the end of a 50–100 ms step depolarization. Inactivation was relieved at +20 mV, while the size of the current remained constant and the speed of Ca^{2+} channel activation increased further. The disappearance of Ca^{2+} current inactivation at potentials positive to +10 mV was probably due to the presence of a slowly increasing inward Ca^{2+} current that overlapped with the decaying phase to give a sustained current of reduced inactivation.

The existence of the slowly activating component was evident when Ca^{2+} was replaced by Ba^{2+} in the external medium (Fig. 1B) (see also Fenwick et al. 1982). HVA Ba^{2+} currents activated and reached maximal amplitudes at more negative potentials (0 mV) than Ca^{2+} currents and reversed at +60 mV (filled circles in Fig. 1C). On average, Ba^{2+} currents were about 2·5-fold larger than Ca^{2+} currents and exhibited little or no sign of time-dependent inactivation. Ba^{2+} currents activated more slowly than Ca^{2+} currents and often showed a double exponential time course of activation, with fast and slow components of very different

time constants. In seven cells, the fast component had a maximal τ_{act} of 3·8 ms at −10 mV (filled circles in Fig. 2A) that was larger than in 10 mM Ca^{2+} (2·3 ms at 0 mV, open circles in Fig. 2A) and larger than τ_{act} reported in bovine chromaffin cells bathed in 5 mM Ba^{2+} (1·8 ms at 0 mV, dashed line in Fig. 2A; Fenwick et al. 1982). Also consistent with this was the rate of Ca^{2+} channel deactivation observed on repolarizations to −50 mV following short depolarizations to 0 mV (Fig. 2B and C). In five cells, τ_{deact} was slower in 10 mM Ba^{2+} (0·38 ± 0·04 ms) than in 10 mM Ca^{2+} (0·25 ± 0·04 ms) (see also Swandulla & Armstrong, 1988).

The time course and voltage dependence of the slowly activating component was estimated best by curve fitting, with double exponential functions, the time courses of both the fast (τ_{act}) and the slow (τ_{slow}) activation phases using long depolarizing pulses (> 150 ms). Figure 3 shows two extreme examples of prolonged HVA currents during pulses to 0 mV. An example of the most frequent case is given in Fig. 3A. The slow component was clearly visible in Ba^{2+}-containing solutions (traces 1 and 3), whereas it was absent when Ca^{2+} replaced Ba^{2+} in the bath (trace 2). In this case,
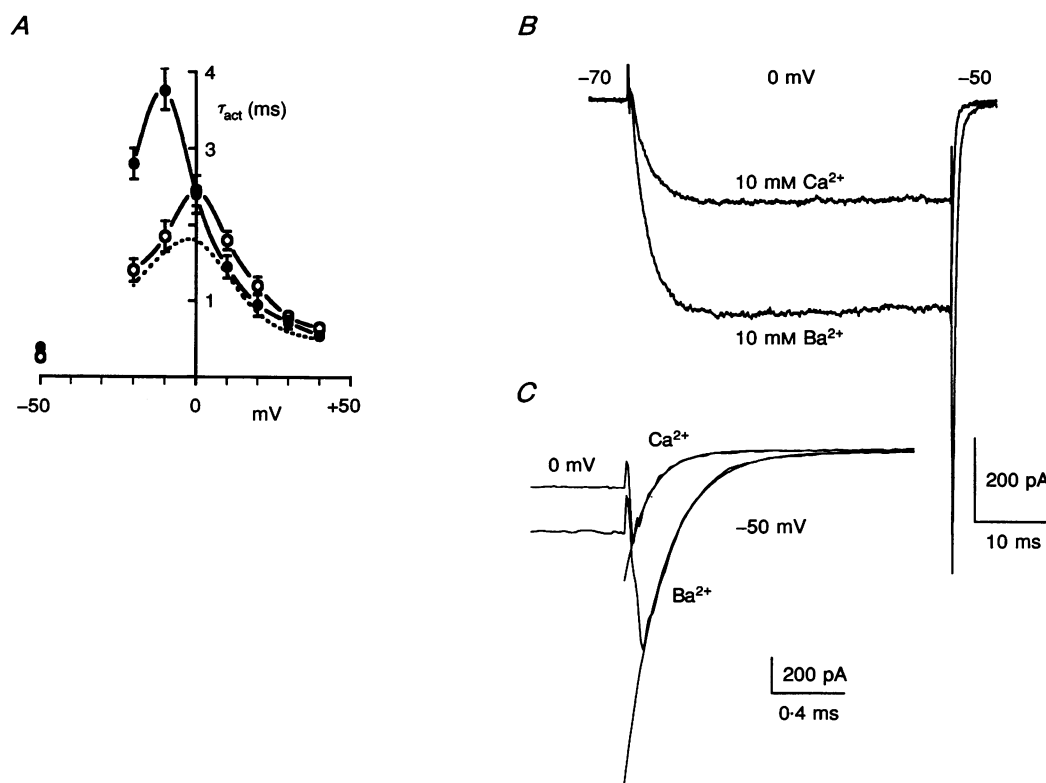

Figure 2. Activation and deactivation characteristics of HVA currents in cat chromaffin cells

A, average time constant of activation (τ_{act}) versus voltage in 10 mM Ba^{2+} (●) and 10 mM Ca^{2+} (○) obtained, in each case, from 7 cells. The dashed line represents the $\tau_{act}(V)$ curve derived from Fenwick et al. (1982) from bovine chromaffin cells bathed in 5 mM Ba^{2+}. The two points at −50 mV are the average τ_{deact} obtained from $n = 3$ cells. B, the two traces were recorded from the same cell perfused first with 10 mM Ca^{2+} and then with 10 mM Ba^{2+} solutions. Test depolarizations were to 0 mV as indicated. V_h was −70 mV. C, tail currents of panel B on a more expanded time scale. Step repolarization was to −50 mV. The two tails were fitted with a single exponential function with $\tau_{deact} = 0·26$ ms (10 mM Ca^{2+}) and 0·41 ms (10 mM Ba^{2+}).

τ_{slow} was 94 ms but values varied considerably from cell to cell (mean, $36\cdot8 \pm 9\cdot2$ ms; $n = 8$). The example shown in Fig. 3*B* occurred less frequently but nevertheless is worthy of mention. With the exception of a slight reduction of HVA current inactivation in Ba^{2+}-containing solutions (trace 2), there was no clear sign of slowly activating components with either Ca^{2+} or Ba^{2+}.

The presence of the slowly activating component introduced some degree of complication to the analysis of Ca^{2+} channel activation kinetics. The slow phase was clearly voltage dependent. The rate of rise of this component increased steeply with voltage. τ_{slow} decreased from $36\cdot8$ ms at 0 mV to $12\cdot5 \pm 3\cdot3$ ms at $+20$ mV ($n = 8$) and to $6\cdot8 \pm 2\cdot3$ ms at $+40$ mV, with a voltage dependence of $17\cdot5$ mV for an e-fold change in the membrane potential. This is comparable to the voltage dependence of the slowly activating component observed in normal sympathetic neurones (Ikeda, 1991) or induced by endogenous neuro-transmitters and intracellular GTP-γ-S in other peripheral neurones (14 mV for an e-fold change) (Marchetti, Carbone & Lux, 1986; Pollo *et al.* 1992; see Discussion).

Sensitivity of HVA currents to Bay K 8644

To test how the DHP agonist Bay K 8644 affected HVA currents, cells were subjected to a series of depolarizing pulses of increasing amplitude before and during application of 1–3 μM Bay K 8644. As in bovine chromaffin cells (Ceña *et al.* 1989; Bossu *et al.* 1991*a*; Artalejo *et al.* 1991*a*), Bay K 8644 also produced a marked potentiation of

HVA currents in cat chromaffin cells. The DHP agonist enhanced the size of the currents, and prolonged the time course of tail currents on repolarization to negative potentials, where normal channels deactivate readily (-50 mV). The increase in current was more evident at low membrane potentials (-40 to -20 mV) at which, in most cases, the agonist increased the size of the currents 3- to 5-fold, and caused deactivations that were approximately 10- to 20-fold slower than control (Fig. 4). There was, however, a significant variability in the action of Bay K 8644; this was attributed to a different distribution of DHP-sensitive and DHP-insensitive Ca^{2+} channels among cat chromaffin cells. In some cells the action of Bay K 8644 was moderate (50 % HVA current increase at -20 mV), despite the large size of the control current. Deactivation in these cells was biexponential and dominated by a fast-decaying component with a time constant that varied between $0\cdot3$ and $0\cdot5$ ms at -50 mV, while the slow component, associated with Bay K 8644-modified channels, had a time constant that varied between 6 and 10 ms and contributed to not more than 25 % of the total tail current. In other cells the current increase induced by the agonist was so evident that it was visible even at the very negative potentials at which channels are usually closed (-50 mV). Tail currents at this potential were dominated by a very slow time course with $\tau_{deact} > 10$ ms. The I–V curves in Fig. 4, inset, were derived from ten cells, bathed in 10 mM Ba^{2+}, that exhibited strong sensitivity to Bay K 8644. The mean Ba^{2+}
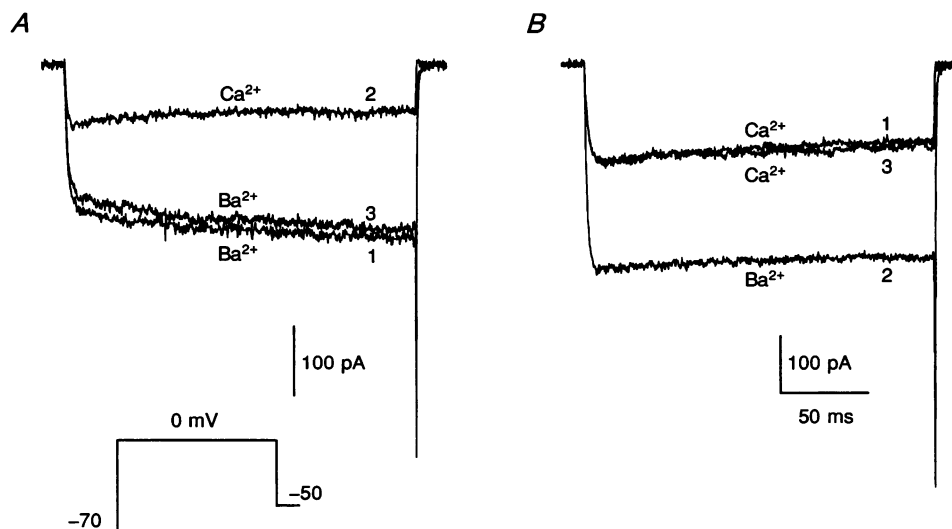

Figure 3. Inactivation of HVA currents during prolonged depolarizations in solutions containing Ca²⁺ or Ba²⁺

A, the cell was perfused sequentially with Ba^{2+} (trace 1), Ca^{2+} (trace 2) and Ba^{2+} again (trace 3). The time constants of the fast and slow activation components (τ_{act}, τ_{slow}) were determined by fitting the time course of Ba^{2+} currents at 0 mV with a double exponential function. Fit limits were set at $0\cdot2$ ms after pulse onset and 1 ms before pulse offset. *B*, a different cell was perfused with Ca^{2+} (trace 1), Ba^{2+} (trace 2) and Ca^{2+} again (trace 3). Test potential was 0 mV and lasted 200 ms in both cases. V_h was -70 mV. Recordings were separated by 30 s intervals.

current amplitude at -20 mV was 152 ± 14 pA in control conditions (filled circles in Fig. 4, inset), and increased to 341 ± 38 pA in the presence of Bay K 8644 (open circles), while τ_{deact} at -50 mV increased from 0.44 ± 0.03 to 9.4 ± 0.6 ms in the presence of the agonist. When Ba^{2+} was replaced by Ca^{2+} in the bath, τ_{deact} of Bay K 8644-modified currents was nearly halved, reinforcing the view that activation–deactivation kinetics of HVA channels can be affected significantly by the divalent permeant cation (Swandulla & Armstrong, 1988).

The presence of a significant fraction of DHP-resistant channels in cat chromaffin cells that activate at slightly more positive potentials than L-type channels was also suggested by the observation that the time course of the tail currents changed depending on the potential at which Ca^{2+} channels were activated. As shown in Fig. 4, in the presence of Bay K 8644, test depolarizations to low membrane potentials (-40 to -20 mV) were usually followed by slow monoexponential tails that reflected the deactivation of a rather homogeneous class of Bay K 8644-modified channels ($\tau_{slow} = 3.9 \pm 0.3$ ms at -50 mV in

10 mM Ca^{2+}; $n = 4$) that start to activate at very negative potentials with half-maximal activation at -41 mV (dashed curve in Fig. 4, inset). In contrast, tail currents following test depolarizations to more positive potentials ($+20$ to $+40$ mV) were best fitted unequivocally by double exponentials with fast and slowly decaying components of comparable size. On return from $+20$ mV, the fast component had a mean τ_{fast} of 0.43 ± 0.06 ms ($n = 4$) and contributed to about half of the tail current amplitude. The other half was due to the slowly deactivating component associated with Bay K 8644-modified channels. Thus, as observed for other secretory cells (Pollo, Lovallo, Biancardi, Sher, Socci & Carbone, 1993) it seems conceivable that besides DHP-sensitive channels, cat chromaffin cells possess, in addition, a set of DHP-insensitive channels that activate at slightly more positive voltages (> 0 mV) and deactivate quickly in the presence of Bay K 8644.

Effects of DHP antagonists

Nisoldipine was selected as a representative DHP Ca^{2+} channel antagonist because it had proved to be an effective
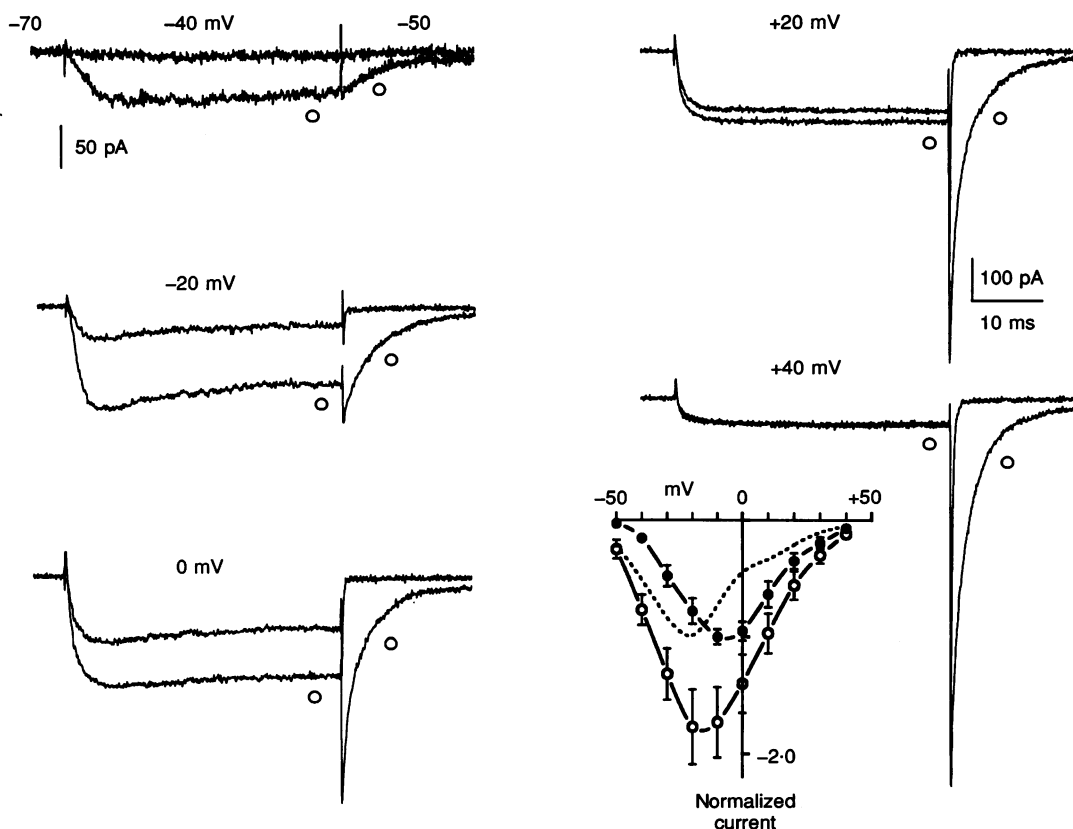

Figure 4. Voltage dependence of Bay K 8644 action on HVA currents of cat chromaffin cells
Current traces recorded before and during (O) application of 3 μM Bay K 8644. Pulses were sequentially applied at 15 s intervals. Notice the time-dependent inactivation of HVA Ca^{2+} currents at -20 and 0 mV that is virtually absent at $+20$ and $+40$ mV. V_h was -70 mV. Inset in the lower right part of the figure shows the I-V curves of peak Ba^{2+} currents in control conditions (●) and in the presence of Bay K 8644 (O). The dashed curve represents the I-V relationship of Bay K 8644-sensitive channels obtained by subtracting Bay K 8644-modified currents from control. Data were normalized as the percentage of the peak current in control conditions at -10 mV and plotted as means $\pm$ S.E.M. of 10 cells bathed in 10 mM Ba^{2+}.

blocker of K^+-evoked secretion in cat adrenal glands (Gandía, López, Fonteríz, Artalejo & García, 1987). When applied to cells bathed in 10 mM Ba^{2+}, nisoldipine (3 μM) depressed the size of HVA currents reversibly during short depolarizations to 0 mV (Fig. 5A). This nisoldipine block had almost no effect on the time course of activation of Ba^{2+}, increased with increasing concentration of DHP and was shown to saturate between concentrations of 1 and 3 μM. Nisoldipine was found to be no more effective at 10 μM than at 3 μM in blocking HVA Ba^{2+} currents. On the other hand, DHP antagonists at concentrations greater than 10 μM were avoided on purpose since they have been reported to block Na^+ and K^+ channels, as well as non-L-type Ca^{2+} channels, in a variety of preparations (Regan, Sah & Bean, 1991). At saturating doses (3 μM), nisoldipine blocked 34 ± 4 % ($n = 34$) of the HVA currents during the first 30 ms of a step depolarization to −10 mV. The nisoldipine block required 20–40 s to be completed and a washing period of 3–4 min for the cells to attain full

recovery. Effects similar to nisoldipine were obtained using other DHP Ca^{2+} antagonists such as nifedipine and furnidipine.

As with other DHPs, the nisoldipine block developed in a time-dependent manner and was more prominent at more negative test potentials (Cohen & McCarthy, 1987; Pollo *et al.* 1993). The time dependence of the DHP block was evident during prolonged step depolarizations (0·6–1 s) to 0 mV. At a concentration of 3 μM, nisoldipine block of open Ca^{2+} channels developed slowly with time, and reached maximal values at about 600 ms from the onset of the pulse (see below and Fig. 7B). In five cells tested, nisoldipine blocked 53 ± 6 % of the sustained HVA current at the end of the pulse to 0 mV and only 28 ± 6 % of the peak current at 20 ms from the onset. In addition, the percentage of the nisoldipine block varied depending on the test potentials. The block was maximal between −30 and −20 mV (73 ± 7 %; $n = 5$) and decreased to about 10 % above +20 mV (Fig. 5B). As a consequence, the I–V
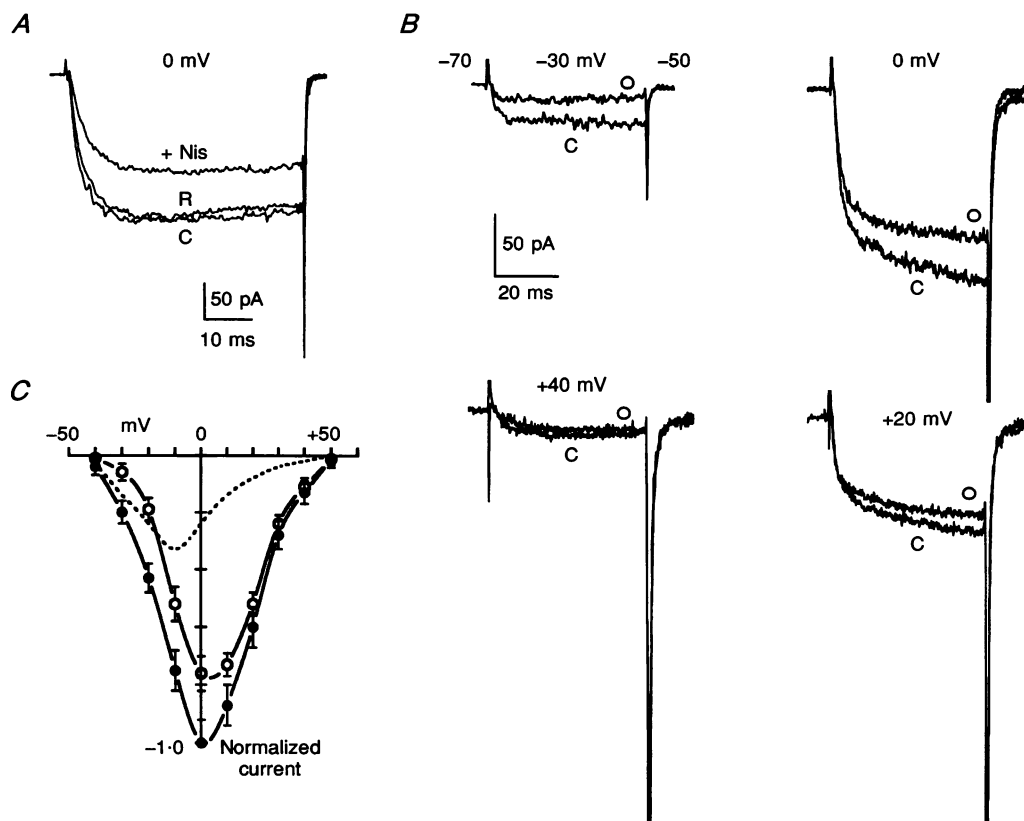

Figure 5. Voltage dependence of the effects of nisoldipine on HVA Ba^{2+} currents

A, three 50 ms test depolarizations to 0 mV, from a V_h of −70 mV, were applied sequentially to a cat chromaffin cell. The current traces were recorded before (control, C), during (Nis) and after (recovery, R) application of 3 μM nisoldipine. B, currents were recorded before (C) and during (O) application of 3 μM nisoldipine at the potentials indicated. Notice the marked block of HVA currents at −30 mV and the reduced effects at +20 and +40 mV. V_h was −70 mV. C, I–V plot at control (●) and in the presence of 3 μM nisoldipine (O). Data represent normalized HVA Ba^{2+} currents measured at the end of each test depolarization of 40 ms. They are plotted as means ± s.e.m. from 5 cells. The dashed curve represents the I–V relationship of DHP-sensitive currents obtained by subtracting DHP-resistant from control currents.

A. Albillos and others

relationship of nisoldipine-resistant currents (half-maximal activation at −15 mV, open circles in Fig. 5C) was slightly shifted from the *I–V* curve of nisoldipine-sensitive currents that activate at more negative membrane potentials (half-maximal activation at −28 mV, dashed line in Fig. 5C). Thus, L-type channels in cat chromaffin cells appear to activate at voltages 13 mV more negative than DHP-resistant channels (mostly N-type), and at voltages 13 mV more positive than L-type channels modified by Bay K 8644 (Fig. 4, inset).

The block of HVA currents by nisoldipine was more effective when the holding potential (V_h) was lowered from −70 to −50 mV. Control HVA currents, during short depolarizing pulses, decreased by $35 \pm 9\%$ ($n = 8$) with little change to their activation–inactivation kinetics, while the nisoldipine block at 0 mV increased by $25 \pm 11\%$, suggesting the presence of an increased fraction of DHP-sensitive channels at a lower V_h.

Tail currents, after short depolarizations to 0 mV, were little affected by nisoldipine. This was probably due to our inability to resolve time course differences from tails that differed by less than 25% in size. A more significant deviation was expected after long depolarizations in which the nisoldipine block could fully develop (53%). In this
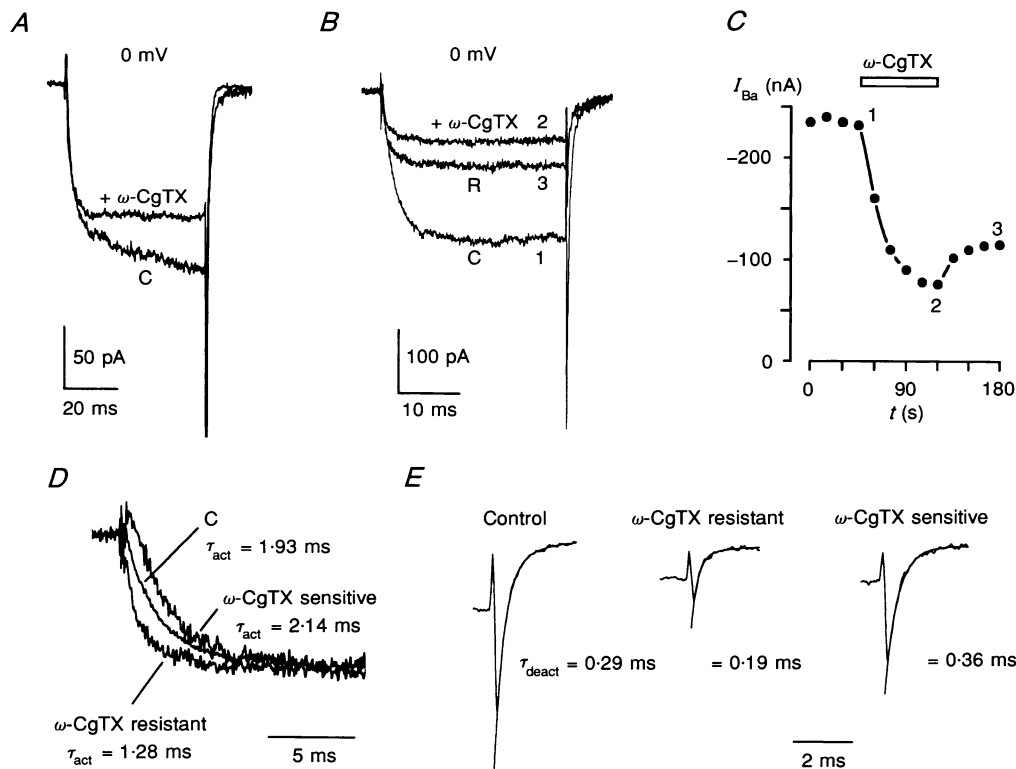

Figure 6. Effects of ω-CgTX on the activation–deactivation kinetics of HVA currents of cat chromaffin cells

A, overlapped current traces recorded at 0 mV from two cat chromaffin cells isolated from the same gland: a normal cell (control, C) and a cell pre-incubated for 4 h in a DMEM solution containing 0·1 μM ω-CgTX (see Methods). Notice the lack of slowly activating components in the trace recorded from the ω-CgTX-treated cell. V_h was −70 mV. *B*, blocking action of ω-CgTX (2 μM) on a cat chromaffin cell bathed in 5 mM Ba^{2+}. The three traces were recorded on step depolarizations to 0 mV in control conditions (trace 1), during application of the toxin (trace 2) and after 3 min wash (R, trace 3). V_h was −70 mV. *C*, time course of peak Ba^{2+} currents recorded at 0 mV from the same cell as in *B*. The bar and numbers indicate the interval of ω-CgTX application and the time at which the traces shown in *B* were recorded. *D*, normalized Ba^{2+} currents recorded at control (C), after ω-CgTX application (ω-CgTX resistant) and their difference (ω-CgTX sensitive) on a more expanded time scale. The ω-CgTX-resistant current (trace 3 in *B*) was scaled to the control current (trace 1 in *B*) by a factor of 2·07. The ω-CgTX-sensitive current (trace 1 − 3) was scaled by a factor of 1·95. The τ_{act} of the three currents are indicated. *E*, time course of tail currents at −50 mV of control, ω-CgTX-resistant and ω-CgTX-sensitive currents. The three tails were fitted by double exponential functions in which the fast component was dominant (85% of the total) and gave values of τ_{deact} as indicated. Given the comparable τ_{deact} of the ω-CgTX-resistant and ω-CgTX-sensitive components (0·19 *versus* 0·36 ms), a more rigorous approach using double exponential fits to resolve these two fast components in the control record (τ_{deact}, 0·29 ms) was found to be of little use.

case, however, our data did not allow a detailed analysis of the time course of the tails to be performed.

ω-CgTX-sensitive currents

The sensitivity of HVA currents to ω-CgTX was tested either by acute or chronic application of the toxin. In chronic experiments the cells were pre-incubated for 20 min to 4 h in a DMEM solution containing 2 mM Ca^{2+} and variable toxin concentrations (0·1–2 μM). The residual currents in ω-CgTX-treated cells had amplitudes 30–40 % smaller than normal, activated at slightly more negative potentials, and often lacked the slow-activation phase that was evident in normal cells at around 0 mV (Fig. 6A).

Acute application of the toxin (1–2 μM) produced a rapid,

but variable, percentage of current depression in nearly all the cells tested. In twelve cells the toxin blocked 46 ± 12 % of the currents. In three of these cells the block was marked and irreversible (73 %) while in the remaining nine cells the depression was partly reversed during wash-out of the toxin (Fig. 6B). The percentage of reversibility of the block varied from cell to cell but never exceeded 30 % of the blocked fraction. In most cases, the degree of reversibility appeared to be limited by Ca^{2+} channel run-down. Depression of HVA currents by 2 μM ω-CgTX, dissolved in 5 mM Ba^{2+}, developed with time constants of 22 ± 3 s (n = 5) and reached steady-state blocking conditions within 90 s (Fig. 6C). The partial wash-out also occurred rapidly and was complete within 60–90 s.
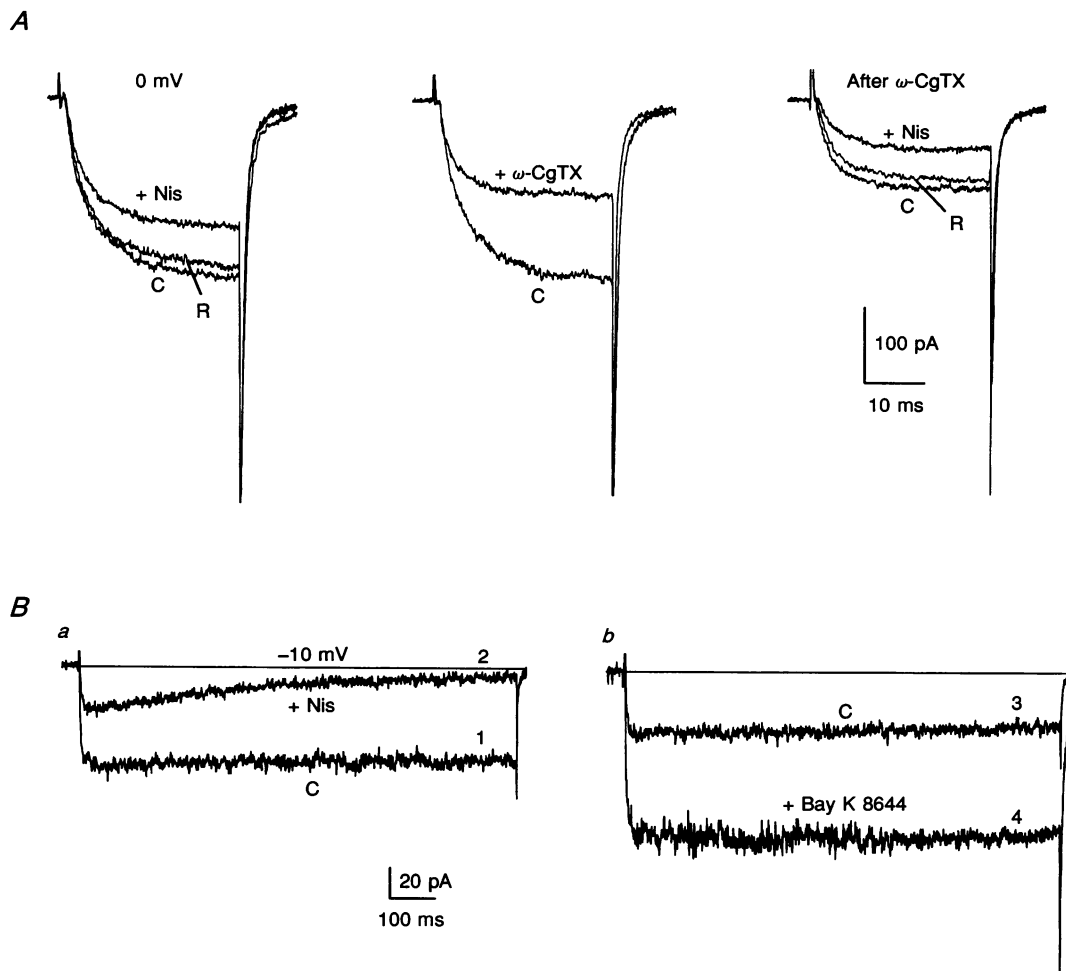

Figure 7. Blocking action of sequentially applied nisoldipine and ω-CgTX on HVA currents

A, test potentials to 0 mV (from a V_h of −70 mV; left traces) were applied before (control, C), during application of 3 μM nisoldipine (Nis) and after a 3 min wash (recovery, R). The middle traces show the control Ba^{2+} current (C) and its partial blockade by ω-CgTX (2 μM for 3 min). Right traces show the effects of nisoldipine (3 μM) on ω-CgTX-resistant currents following the same protocol used for the middle trace. B, long-lasting HVA current recordings on a cell pretreated with ω-CgTX. Nisoldipine (3 μM) caused a slow but complete block of ω-CgTX-resistant channels that were activated at −10 mV (trace 2 in a). Following recovery (trace 3 in b) application of Bay K 8644 (1 μM) produced a marked enhancement of the ω-CgTX-resistant current (trace 4), suggesting a dominance of L-type channels in ω-CgTX-treated cat chromaffin cells.

The application of ω-CgTX induced clear changes in the kinetics of activation and deactivation of HVA currents. ω-CgTX-resistant currents (trace 3 in Fig. 6B) were shown to activate and deactivate faster than control currents (trace 1). At 0 mV, τ_{act} decreased from $2\cdot3 \pm 0\cdot2$ ms to $1\cdot5 \pm 0\cdot3$ ms ($n = 5$) after treatment with ω-CgTX, while τ_{deact}, on return to -50 mV, decreased from $0\cdot33 \pm 0\cdot05$ ms to $0\cdot21 \pm 0\cdot03$ ms ($n = 5$) after toxin application (Fig. 6D and E). The time courses of activation and deactivation of the ω-CgTX-sensitive component (traces 1–3) are also

illustrated in Fig. 6D and E; these differ very little from the control (τ_{act}, $2\cdot5 \pm 0\cdot3$ ms; τ_{deact}, $0\cdot36 \pm 0\cdot05$ ms).

The depression of HVA currents by DHPs occurred independently of the action of ω-CgTX. Figure 7A shows an example of the blocking action of 3 μM nisoldipine before and after ω-CgTX application to a cat chromaffin cell bathed in 10 mM Ba²⁺. The amount of current blocked by nisoldipine before and after toxin application is nearly preserved (45 *versus* 40 pA; Fig. 7A). In percentage terms, however, the nisoldipine block after toxin application was
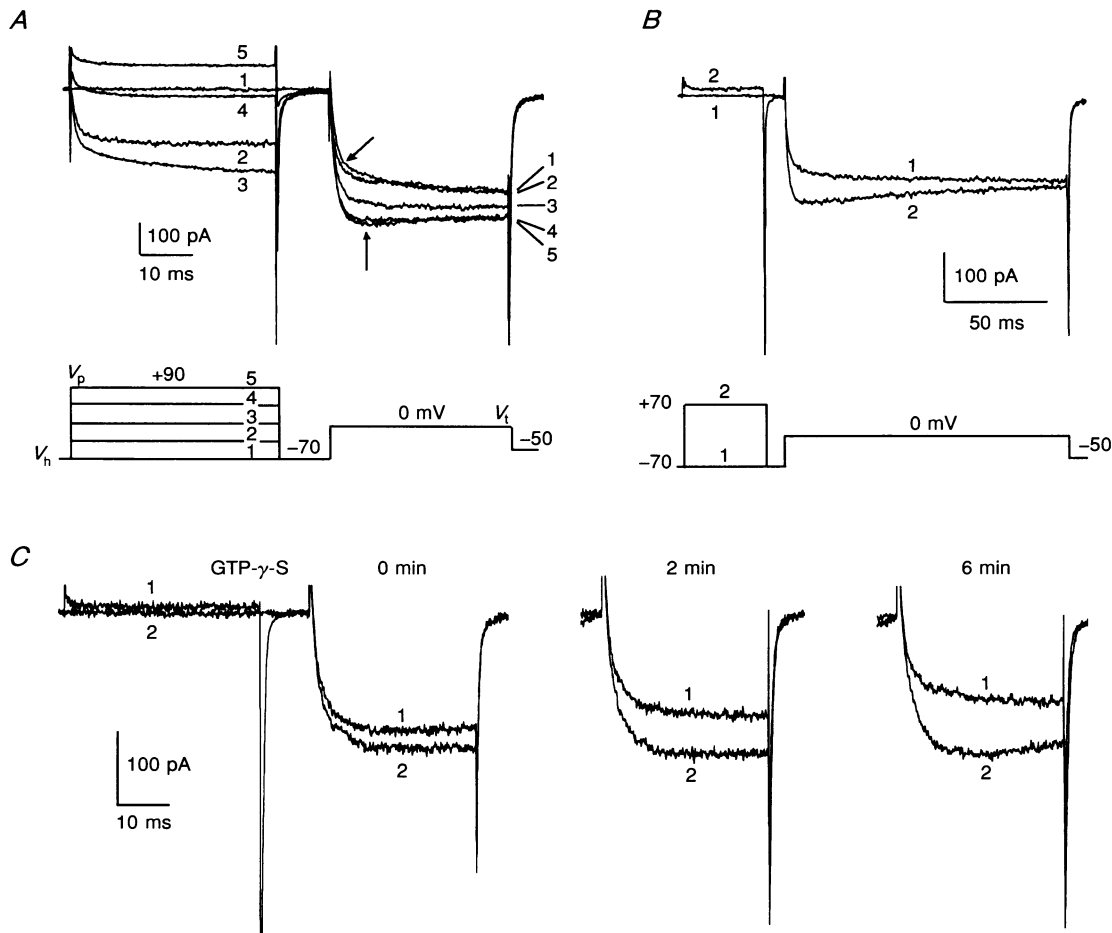

Figure 8. Facilitation of HVA Ba²⁺ currents in cat chromaffin cells is voltage dependent and enhanced by intracellular GTP-γ-S

A, facilitation of HVA Ba²⁺ currents by conditioning prepulses of varying amplitude. Prepulses (V_p) of increasing amplitude were applied from V_h with step increments of 40 mV. A 10 ms repolarization to V_h was allowed before applying a constant test pulse to 0 mV (V_t). Facilitation consisted of a current amplitude increase (traces 3–5) and of the disappearance of the slow activation phase, visible only in traces 1 and 2. Maximal facilitation was observed with prepulses > $+50$ mV (traces 4 and 5). The two arrows indicate the times at which the HVA current amplitude was measured, with and without prepulses, to derive the percentage of prepulse-induced facilitation. B, time course of the facilitated current during prolonged test pulses (140 ms). Traces 1 and 2 were recorded sequentially without (1) and with (2) a pre-depolarization of 40 ms to $+70$ mV as indicated. Notice the pronounced inactivation on the facilitated current that slowly relaxes back to its control level. C, prepulse-induced facilitation in the presence of GTP-γ-S (100 μM) in the intracellular solution. The first recordings, on the left, were taken soon after breaking into the cell ($t = 0$). The other traces were recorded 2 and 6 min later, as indicated. The pulse protocol was similar to that of A, with $V_p = +70$ mV, $V_h = -70$ mV and $V_t = 0$ mV.

larger than in normal cells, with a mean current depression of $55 \pm 4\%$ at 0 mV ($n = 18$), independent of whether the cell was acutely or chronically treated. More striking was the time-dependent block of HVA currents in ω-CgTX-treated cells during long-lasting depolarizations (Fig. 7B). The nisoldipine block of open HVA channels developed with a τ_{block} of 287 ms (mean, 437 ± 98 ms; $n = 6$) and was nearly complete after a 1 s step depolarization to -10 mV (trace 2 in Fig. 7Ba). Despite the long depolarizations, the action of nisoldipine could be largely reversed on washing out (trace 3). Subsequent addition of Bay K 8644 (1 μM) caused a 2·8-fold increase of Ba^{2+} currents (trace 4), indicating a dominance of L-type Ca^{2+} channels in ω-CgTX-treated cat chromaffin cells. Alternatively, it could be concluded that ω-CgTX-sensitive channels represent the dominant fraction of DHP-resistant currents in cat chromaffin cells.

Facilitation of HVA currents by depolarizing prepulses

Facilitation of Ca^{2+} currents by depolarizing prepulses in bovine chromaffin cells has been reported consistently by several groups (Fenwick *et al.* 1982; Hoshi, Rothlein & Smith, 1984; Hoshi & Smith, 1987; Artalejo *et al.* 1991a). We thought it would be interesting, therefore, to test whether cat chromaffin cells also exhibited this property. Prepulse-induced facilitation in our cells was evident using the pulse protocol illustrated in Fig. 8A. A constant test depolarization to 0 mV (V_t) was preceded by a conditioning prepulse of 40 ms to various potentials (V_p) and by a 10 ms repolarization to V_h. Under these conditions, V_p of increasing amplitudes produced a progressive increase of the Ba^{2+} current at V_t (traces 1–5) that reached maximal amplitude above $+50$ mV (traces 4 and 5). Usually, the current
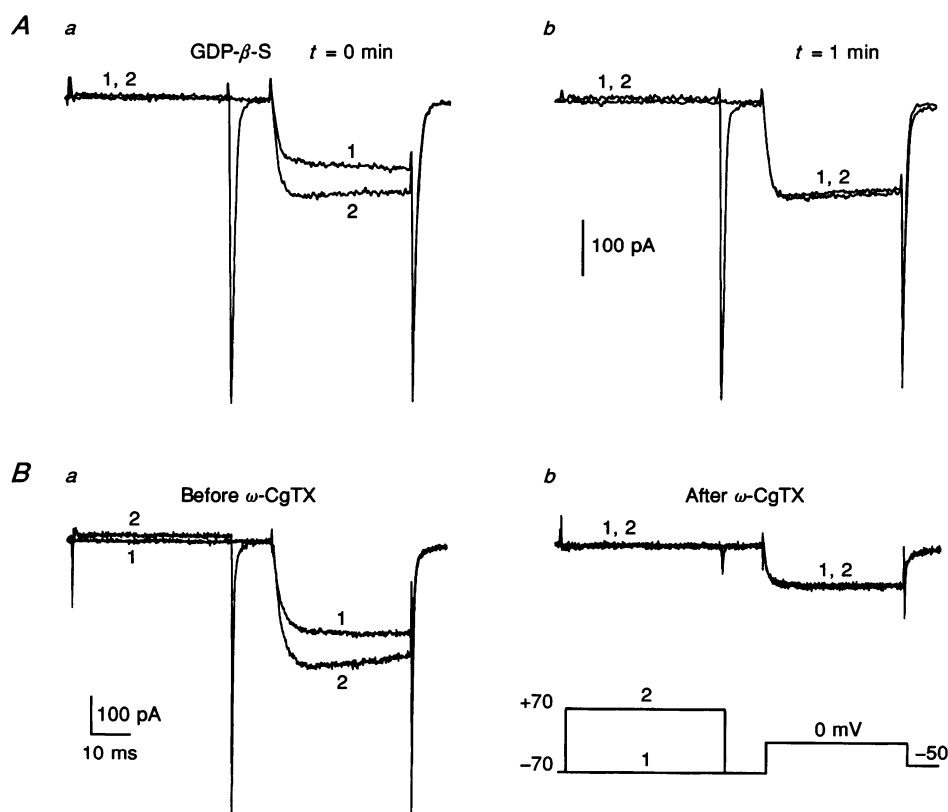

Figure 9. Intracellular GDP-β-S and externally applied ω-CgTX abolish prepulse-induced facilitation in cat chromaffin cells

A, prepulse-induced facilitation recorded from a cell perfused with 1 mM GDP-β-S in the pipette solution, soon after establishing the whole-cell recording conditions ($t = 0$ min; *a*) and 1 min later (*b*). Notice the full disappearance of facilitation after the short application of GDP-β-S. *Ba* shows control HVA currents recorded from a different cell without (trace 1) and with (trace 2) a prepulse of 40 ms to $+70$ mV from $V_h = -70$ mV. Notice the marked facilitation at 0 mV induced by the positive prepulse (trace 2). Records in *Bb* were obtained using the same pulse protocol but after a 2 min application of 2 μM ω-CgTX and 2 min wash. The toxin was dissolved in a solution containing 5 mM Ba^{2+}. Prepulse-induced facilitation was fully prevented by the toxin.

increase induced by a prepulse of 50 ms to +70 mV was found to be proportional to the size of the slowly activating component of the control current and could be expressed, therefore, as a percentage of the current amplitude at 0 mV. In seventeen cells, maximal facilitation induced a $37 \pm 2\%$ increase in the current size, measured as illustrated in Fig. 8A (see legend). With the exception of a change in the activation kinetics (see below), the percentage of facilitation was unaffected if Ba^{2+} was replaced by Ca^{2+}. This indicates a close correlation, and a probable common origin, between facilitated and normal currents that were both halved when cells were bathed in 10 mM Ca^{2+} solution. In addition, the observation that the time course of the tail currents at -50 mV does not change substantially after the prepulse is consistent with this idea (Fig. 8A), suggesting that the deactivation of facilitated currents is not significantly different from that of control currents (see also Figs 9 and 10).

Facilitation by prepulses changed the time course of Ba^{2+} current activation markedly. After strong preconditioning pulses the slow phase of Ba^{2+} current activation disappeared. The facilitated currents peaked between 3 and 4 ms after the onset of V_t and then declined towards the end of the pulse (trace 5 in Fig. 8A). Prolonged test depolarizations

(140–200 ms) showed clearly that the inactivating phase, induced by strong prepulses, reflects a slow return of the facilitated current to control levels (Fig. 8B). In most cells, facilitated and control currents approached the same steady-state level after approximately 120 ms. Facilitation depended also on the length of the prepulse. In two cells we found that maximal facilitation at +70 mV was achieved just after a prepulse duration of 20 ms (not shown). Thus, voltage-dependent facilitation in cat chromaffin cells appears to be controlled by fast molecular events, similar to neurones (Grassi & Lux, 1989; Elmslie, Zhou & Jones, 1990; Pollo et al. 1992).

This view was also strengthened by the observation that intracellular application of GTP-γ-S (100 μM) preserved and potentiated prepulse-induced facilitation (Fig. 8C). In seven cells, the degree of facilitation in the presence of GTP-γ-S increased progressively with time to reach maximal values after 3–5 min (mean, $53 \pm 4\%$). After that, facilitation remained constant for several minutes and, in some cases, could be maintained for up to 20 min with little loss of total current. In contrast, however, internal application of GDP-β-S (0·5–1 mM) completely prevented prepulse-induced facilitation within 1–2 min ($n = 10$; Fig. 9A). Also consistent with this was the observation that
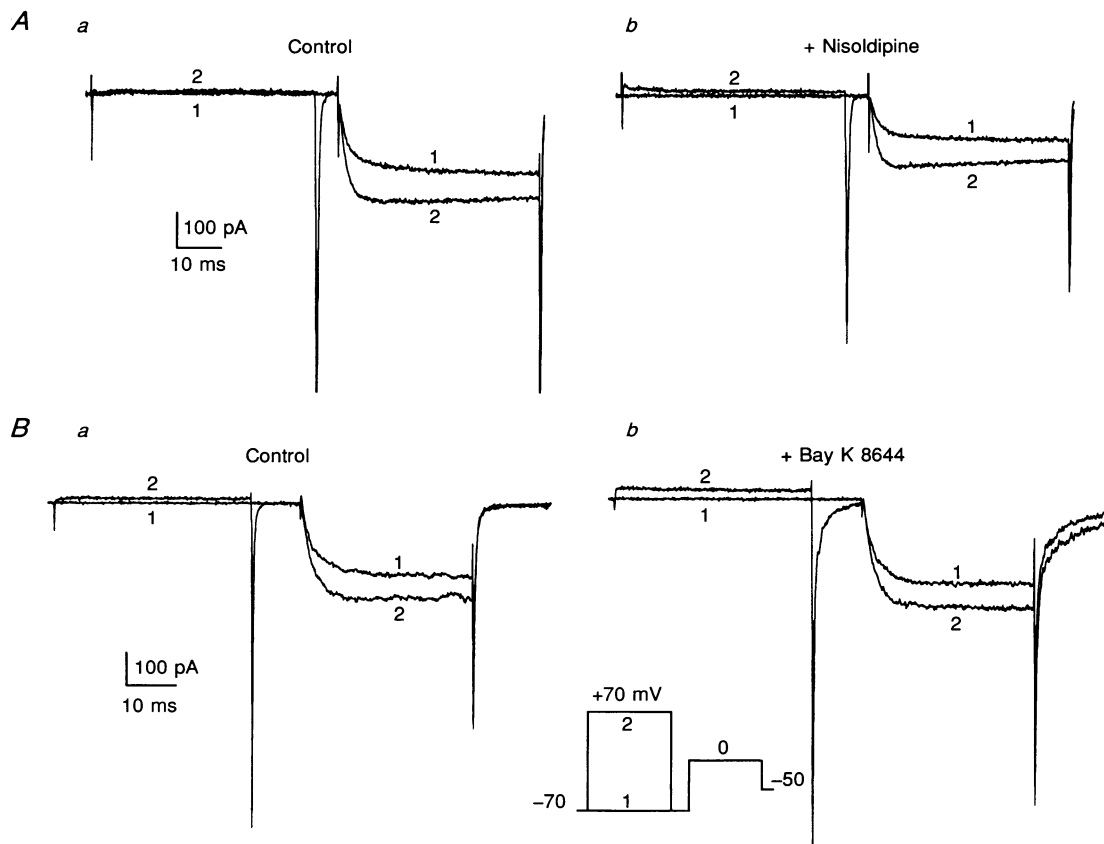

Figure 10. Prepulse-induced facilitation in cat chromaffin cells is little affected by nisoldipine and Bay K 8644

Nisoldipine (3 μM; A) and Bay K 8644 (3 μM; B) were applied for 3 min in 10 mM Ba^{2+} before recording the two traces shown in A b and B b. The pulse protocol was similar to that of Fig. 9B.

cells perfused with a GTP-free internal solution showed, initially, a small prepulse-induced facilitation (12 ± 3 %, n = 6) that was reduced further during cell dialysis.

To assay the pharmacology of Ca²⁺ channel subtypes underlying the facilitated current, we tested its sensitivity to ω-CgTX and DHPs. As shown in Fig. 9B, ω-CgTX was very effective in depressing the size of normal HVA Ba²⁺ current and the corresponding facilitated current. This feature was observed in twelve out of fourteen ω-CgTX-treated cells in which the facilitation was depressed by 87 ± 4 %. In the remaining two cells, ω-CgTX only partly reduced the percentage facilitation, although it depressed the size of the total current by 45 % . In these two cases, however, we were unable to discriminate between whether the current depression was due to a rapid Ca²⁺ channel rundown while the toxin was applied, or to the true action of the toxin.

In contrast to ω-CgTX, nisoldipine had only a weak effect on the prepulse-induced facilitation despite the fact that, in some cases, nisoldipine blocked a significant fraction of the control current (Fig. 10A). In twenty-one out of twenty-five cells, the DHP depressed the total current by 31 ± 5 % but depressed the corresponding prepulse-induced facilitation by less than 5 %. In the remaining four cells, however, the DHP had moderate inhibitory effects on the facilitation current (a reduction of 23 ± 3 %) suggesting some minor contribution of L-type channels to this current. In addition, Bay K 8644 had minor effects on the facilitation current induced by the prepulse, although the DHP agonist was able to increase the size of the current and to prolong its tail under control conditions. In fourteen cells, the 35 ± 4 % increase in current due to prepulse-induced facilitation was neither reduced nor enhanced by 1–3 μM Bay K 8644 (Fig. 10B). We could, however, observe a slight increase in the slow component of the tails suggesting some contribution of slowly deactivating channels after the prepulse, as if the voltage-dependent facilitation could recruit a minor fraction of DHP-sensitive channels which were otherwise unavailable at rest.

DISCUSSION

Catecholamine release from perfused cat adrenal glands is potently inhibited by DHP antagonists when both nicotinic receptor activators (Ladona, Aunis, Gandía & García, 1987) or high K⁺ concentrations (Gandía et al. 1987) are used as secretagogues. One consequence of this is that regulation of secretion in feline chromaffin cells is likely to be dominated by L-type Ca²⁺ channels, justifying early assumptions that feline chromaffin cells (as opposed to bovine chromaffin cells) could express only one Ca²⁺ channel subtype (see Artalejo et al. 1988). The results of the present investigation demonstrate that, in addition to L-type Ca²⁺ channels, cat chromaffin cells possess at least two other Ca²⁺ channels: an ω-CgTX-sensitive channel (N-type) that accounts for most

of the DHP-resistant current and a DHP- and ω-CgTX-resistant channel that contributes only to a marginal fraction of the total current. Our conclusions are mostly based on pharmacological grounds that can be summarized as follows. (1) Saturating concentrations of nisoldipine and other DHP antagonists only partly block (40–50 %) the size of HVA currents, even during long depolarizations to 0 mV in which L-type channels are fully active. (2) ω-CgTX blocks nearly half of the currents in a partly reversible manner. (3) Nisoldipine and Bay K 8644 are more effective after ω-CgTX application, and appear to be additive to the inhibitory effects of the toxin. (4) Sequential applications of DHP antagonists and ω-CgTX leave unaltered a small residual current that may be associated with a third, not well identified, HVA Ca²⁺ channel subtype. (5) The current facilitation induced by conditioning prepulses is due to a fast, voltage-dependent recruitment of a large fraction of ω-CgTX-sensitive channels (N-type) together with a minority of L-type channels that are tonically inhibited at rest.

Kinetic properties of Ca²⁺ channels in cat chromaffin cells

As in other cell preparations, separation of Ca²⁺ channel subtypes by their activation–inactivation properties was nearly impossible without the aid of pharmacological tools (see Swandulla, Carbone & Lux, 1991). Above 0 mV, for example, the fast activation time course of the total currents showed little sign of double components. The same was true for the inactivation time course of Ba²⁺ currents which was usually slow and largely incomplete even during long depolarizing pulses (Fig. 7B). The issue of HVA channel inactivation was complicated in any case by the presence of two opposite phenomena: (1) the slow voltage-dependent phase of HVA channel activation that was mostly evident in Ba²⁺ solutions, and could partly compensate the decaying phase of Ca²⁺ channel inactivation; and (2) the time-dependent block of L-type channels by nisoldipine that could be easily confused with an increased time-dependent current inactivation (see Cohen & McCarthy, 1987; Swandulla et al. 1991; Pollo et al. 1993).

Nevertheless, significant kinetic differences could be detected when ω-CgTX or DHP antagonists were applied. As with bovine chromaffin cells, the slow phase of activation was found to be mainly associated with the ω-CgTX-sensitive component (Artalejo, Perlman & Fox, 1992a). Slow activation phases were hardly detected in ω-CgTX-treated cells and were largely unaffected by DHPs. Application of ω-CgTX revealed, in addition, an ω-CgTX-resistant component (mostly L-type) that activates and deactivates about 2-fold faster than the total current (Fig. 6). This agrees with previous observations on bovine chromaffin cells (Artalejo et al. 1992a) and peripheral neurones (Regan et al. 1991; Kasai & Neher, 1992; Pollo et al. 1993), suggesting that ω-CgTX-sensitive and ω-CgTX-resistant channels possess different ranges of voltage

activation and rates of activation–deactivation which are hardly separable by simple kinetic analysis. Recent reports have shown that DHP-sensitive channels in neurones (Carbone *et al.* 1990; Regan *et al.* 1991; Kasai & Neher, 1992), and insulin-secreting cells (Pollo *et al.* 1993), activate at more negative potentials (−30 to −10 mV) than DHP-resistant channels (−20 to 0 mV). We found the same in cat chromaffin cells (Fig. 5*C*) thereby giving a rationale for the more effective action of nisoldipine and Bay K 8644 between −40 and −20 mV, where probably a larger fraction of L-type channels is available for activation. The action of Bay K 8644 is further potentiated by the −10 to −15 mV shift of the *I–V* curve induced by the agonist (Fig. 4, inset).

DHP-sensitive channels

The effects of DHPs observed in cat chromaffin cells are strongly analogous with those reported for bovine chromaffin cells. Hoshi & Smith (1987) reported that Ca^{2+} currents in bovine chromaffin cells were potentiated by 1–5 μM Bay K 8644. The agonist promoted long openings with mean open times as large as 18 ms. Subsequently, prolonged tail currents and corresponding Ca^{2+} current increases were also reported by Ceña *et al.* (1989), Artalejo, Ariano, Perlman & Fox (1990) and Bossu *et al.* (1991*a*) using Bay K 8644 concentrations as low as 0·1–1 μM. Thus, our observation that HVA currents in cat chromaffin cells are also markedly enhanced by DHP agonists suggests that L-type channels might be ubiquitous in a variety of chromaffin cells, and may contribute significantly to the total HVA current. In addition, the existence of mixed populations of DHP-sensitive and DHP-insensitive channels in cat chromaffin cells is supported by the different time courses of tail currents at various test potentials. They are slow (6–10 ms in 10 mM Ba^{2+}) and nearly monoexponential following depolarizations to −40 and −20 mV (Fig. 4) but are best fitted by biexponentials with fast deactivating components after stronger depolarizations. To our knowledge, the Bay K 8644-induced prolongation of tail currents observed in cat chromaffin cells appears more pronounced than that reported for peripheral neurones (Plummer, Logothetis & Hess, 1989; Carbone *et al.* 1990; Regan *et al.* 1991) and insulin-secreting cells (Pollo *et al.* 1993). This might suggest significant differences in the gating and/or Bay K 8644 sensitivity among L-type channels in various tissues.

The effects of DHP antagonists observed in cat chromaffin cells are in good agreement with those of Bossu *et al.* (1991*a*) who reported a marked reduction of Ca^{2+} currents by nicardipine (10 μM) in bovine chromaffin cells. The nicardipine block was accompanied by an increased acceleration of HVA channel inactivation; this is consistent with the observation that 3 μM nisoldipine blocks HVA currents in a time-dependent manner during long-lasting depolarizations in cat chromaffin cells. Our data, however, deviate from those of other reports showing that nisoldipine (1 μM) is ineffective in blocking HVA

currents during short pulses (Artalejo *et al.* 1990), or requires higher doses (10–30 μM) to block 20 % of the currents in bovine chromaffin cells (Gandía, García & Morad, 1993). The probable reason for this is that bovine chromaffin cells express a lower density of L-type channels than cat chromaffin cells (see below). On the other hand, our experiments with 1–3 μM DHP antagonists show clearly that cat chromaffin cells possess a significant fraction of L-type channels that can be largely blocked around 0 mV if the test pulses used last long enough to allow steady-state blocking conditions to be reached (Fig. 7*B*). The action of nisoldipine appears to be particularly potent at low membrane potentials (75 % at −30 mV) and requires several minutes to be washed out. This suggests a high affinity binding for the DHP and an apparently voltage-dependent blocking mechanism that arises from the presence of two sets of HVA channels (DHP sensitive and DHP insensitive) that activate at slightly different membrane potentials (Fig. 5). Time-dependent block of L-type channels by DHP antagonists has also been reported for other secretory cells (Cohen & McCarthy, 1987; Pollo *et al.* 1993) and peripheral neurones (Regan *et al.* 1991). This phenomenon may have been overlooked during previous experiments and could explain some of the contradictions concerning the weak sensitivity of HVA currents to Ca^{2+} antagonists, which are in contrast to the potent effects of Bay K 8644 reported by most authors.

ω-Conotoxin-sensitive channels

The co-existence of ω-CgTX-sensitive channels and L-type channels has been reported consistently in bovine chromaffin cells (Hans *et al.* 1990; Artalejo *et al.* 1992*a*; Gandía *et al.* 1993) and in rat phaeochromocytoma (PC12) cells (Sher, Pandiella & Clementi, 1988; Plummer *et al.* 1989). In bovine cells, the block of HVA currents by ω-CgTX was largely irreversible and varied from cell to cell. On average, however, the toxin blocked approximately half of the currents. In PC12 cells, the block by ω-CgTX was stronger (60–70 %), but partly reversible. The permanently blocked fraction was about 40 % of the total (Plummer *et al.* 1989). Our present data suggest that the action of ω-CgTX on cat chromaffin cells is closer to that observed on PC12 cells. Indeed, we found that the marked block of HVA currents by the toxin was often followed by a partial recovery, but we made no attempt to determine whether the reversibly blocked channels represented a distinct class of ω-CgTX-sensitive (N-type) channels, or a subclass of L-type channels sensitive to ω-CgTX. Given the additive action of DHPs and ω-CgTX (Fig. 7), the only conclusion to be drawn from our present data is that the irreversibly blocked ω-CgTX-sensitive channels are pharmacologically distinct from L-type channels in cat chromaffin cells and that the two sets of channels contribute to the majority of the control currents (85 %). Single channel analysis and other Ca^{2+} channel blockers might help to distinguish the nature of the residual DHP-

and ω-CgTX-resistant current. The contribution of P-type Ca^{2+} channels, as reported in peripheral and central neurones (Mintz, Adams & Bean, 1992) cannot be excluded *a priori*. However, their low density in sympathetic neurones (Mintz *et al.* 1992), and the limited size of residual currents in our cells (10–15 %), would also suggest a marginal contribution, if any, of P-type channels in cat chromaffin cells. Preliminary experiments suggest that ω-agatoxin IVA (300 nm; Peptide Institute, Inc., Osaka, Japan) blocks Ba^{2+} currents in these cells by only 10–15 % (authors' unpublished observations).

Voltage-dependent facilitation of Ca^{2+} currents

Fenwick *et al.* (1982) were the first to observe that strong depolarizing prepulses to positive potentials induce a 25–35 % facilitation of Ca^{2+} currents in bovine chromaffin cells. Hoshi *et al.* (1984) corroborated this observation and showed that the facilitation of Ca^{2+} currents is a voltage-dependent phenomenon independent of Ca^{2+} entry. We also find that depolarizing prepulses of 40 ms to + 70 mV induce a 37 % facilitation of Ba^{2+} currents in feline chromaffin cells (Fig. 8). Facilitation in cat chromaffin cells is also voltage dependent but reaches maximal values with prepulses that are shorter and smaller than those reported for bovine chromaffin cells, namely 70 ms to +80 mV (Hoshi *et al.* 1984) or 200 ms to +120 mV (Artalejo *et al.* 1991*a*). Thus, the facilitation of HVA currents, although exhibiting different kinetics, seems to be a common phenomenon of chromaffin cells in various animal species.

Differences do exist, however, in the pharmacology of the current facilitation. In bovine chromaffin cells, Artalejo *et al.* (1990, 1991*a,b*) interpreted the phenomenon of facilitation in terms of the recruitment, by prepulses, of a current associated with a 27 pS L-type Ca^{2+} channel that is superimposed on a 'standard current'. The standard current is an HVA current, evoked without prepulses, flowing through neither L- nor 'classical' N-type channels. The arguments for this are that the 'facilitated current' is suppressed selectively by 1 μM nisoldipine, and is absent in the presence of 1 μM Bay K 8644 (Artalejo *et al.* 1990). In addition, facilitation appears to be derived from a fast voltage-dependent phosphorylation process that is independent of the activation of G-proteins (Artalejo, Rossie, Perlman & Fox, 1992*b*). At variance with this, the current facilitation in cat chromaffin cells exhibits a strong sensitivity to ω-CgTX, is weakly affected by 3 μM nisoldipine and Bay K 8644, and is regulated by G-protein activation (Figs 8 and 9). Thus, at least in the cat, facilitation seems to be derived from a recruitment of ω-CgTX-sensitive channels that are partly inhibited at rest. This resembles closely the prepulse-induced facilitation observed in tonically inhibited sympathetic neurones (Ikeda, 1991) or, more generally, in neurones in which the HVA current is inhibited by internal GTP-γ-S and externally applied hormones or neurotransmitters (Grassi & Lux, 1989; Elmslie *et al.* 1990;

Pollo *et al.* 1992). In this respect, facilitation with strong prepulses (+50, +70 mV) reflects a quick voltage-dependent recruitment of ω-CgTX-sensitive channels that are inhibited at rest. At mild depolarizations (0, +10 mV), facilitation is slow and gives rise to the slow phase of activation (Fig. 1*B*). Alternatively, the slowly inactivating current observed after facilitation mostly represents the re-establishment of inhibition at these potentials (see the model in Pollo *et al.* 1992). As a consequence of this the 'facilitated current' does not originate from the recruitment of a distinct Ca^{2+} channel that activates transiently after the prepulse, but is derived mostly from ω-CgTX-sensitive channels that recover from a resting inhibition and contribute partly to the control current (Elmslie *et al.* 1990; Swandulla *et al.* 1991).

An important point of our work is that, as in bovine chromaffin cells (Gandía *et al.* 1993) and sympathetic neurones (Ikeda, 1991), G-proteins mediate the voltage-dependent facilitation in cat chromaffin cells. Facilitation is fully and quickly prevented by high doses of the non-hydrolysable GDP analogue, GDP-β-S (1 mm), while the GTP analogue, GTP-γ-S, preserves and potentiates the tonic inhibition of HVA currents, which are facilitated largely by strong depolarizing prepulses (Fig. 8*C*). Thus, there seems little doubt that, as in neurones, facilitation of ω-CgTX-sensitive channels in cat chromaffin cells may be mediated effectively by G-proteins. The issue to be clarified, then, is the possible origin of the tonic inhibition and the related voltage-dependent facilitation. Inhibition of HVA currents, triggered by the release of molecules contained in chromaffin granules (catecholamines, chromogranins, ATP and opiates) or by the sustained production of intracellular GTP might both account for these phenomena. Preliminary data indicate that both μ-opioid agonists and ATP can induce marked voltage-dependent inhibitions of HVA currents in cat chromaffin cells (authors' unpublished observations; see also Gandía *et al.* 1993). Given that catecholamine secretion in bovine chromaffin cells is a fast event, resolved within tens of milliseconds (Chow, Von Ruden & Neher, 1992), and that Ba^{2+}, as well as Ca^{2+}, may trigger exocytosis (Terbush & Holz, 1992), it is conceivable that during the slow perfusion conditions and voltage-clamp recordings used in the present study, an uncontrolled secretion of neurotransmitters and ATP may have taken place at rest, as well as during stimulation, thus triggering the inhibition of tonic Ba^{2+} currents. Future work will help to clarify this issue.

Relevance to the regulation of catecholamine secretion

The presence of multiple Ca^{2+} channels in cat chromaffin cells raises the question of their possible role in the regulation of Ca^{2+} entry during the activation of nicotinic and muscarinic receptors. Early experiments on bovine chromaffin cells demonstrated that nitrendipine effectively blocked the nicotine- and K^+-evoked release of radiolabelled

noradrenaline (Ceña, Nicolás, Sánchez-García, Kirpekar & García, 1983). In later reports, however, the block of catecholamine release by DHPs proved to be partial in both cultured bovine chromaffin cells and intact bovine adrenal glands (Gandía et al. 1990). In contrast, secretory responses in cat adrenal glands always exhibited a high sensitivity to DHP agonists and antagonists (García et al. 1984; Ladona et al. 1987; Gandía et al. 1987; Gandía et al. 1990). High-affinity binding of [^{3}H]nitrendipine in cat adrenal medullary tissue was usually accompanied by a pronounced blockade of ^{45}Ca^{2+} uptake and a marked reduction of catecholamine release in K$^+$-depolarized chromaffin cells, suggesting that L-type Ca^{2+} channels were likely to dominate the control of exocytosis, at least in feline species (Artalejo et al. 1988). One point still to be proved, however, is whether secretion evoked by a more physiological means (such as electrical stimulation of splanchnic nerve terminals) exhibits as high a sensitivity to DHPs as does K$^+$-evoked secretion. In the perfused rat adrenal, for instance, the electrically induced secretion of catecholamines appears to be less sensitive to DHPs than K$^+$-evoked secretion (López, Shukla, García & Wakade, 1992). Thus, under more physiological conditions, non-L- and L-type Ca^{2+} channels might co-operate in controlling exocytosis.

The unequivocal presence of an ω-CgTX-sensitive Ca^{2+} current component raises the question of what the functional role of an 'N-type' channel in cat chromaffin cells might be. Catecholamine secretion in these cells seems to be more complex than in bovine cells. For instance, in the feline gland both nicotinic and muscarinic receptors mediate the secretory response (Douglas & Poisner, 1965), while in the bovine gland, despite the presence of muscarinic receptors, stimulation by muscarinic agonists fails to trigger the release of catecholamines, this release being controlled predominantly by nicotinic receptor stimulation (Ballesta et al. 1989). It is conceivable, therefore, that various Ca^{2+} channel subtypes, with different pharmacology and modulatory properties, may also serve different exocytotic functions in adrenal feline chromaffin cells as compared to bovine species. On the other hand, N-type channels have been implicated in the control of adrenergic receptor-mediated inhibition of noradrenaline release in sympathetic neurones (Hirning et al. 1988). Given the close similarity between sympathetic neurones and chromaffin cells, and the presence of a voltage-dependent facilitatory process on the ω-CgTX-sensitive channel of both cells (Ikeda, 1991), it is probable that N-type channels may also contribute to the regulation of the voltage-dependent catecholamine release in cat chromaffin cells.

REFERENCES

ARTALEJO, C. R., ARIANO, M. A., PERLMAN, R. L. & FOX, A. P. (1990). D1 dopamine receptors activate facilitation Ca channels in chromaffin cells via a cAMP/protein kinase A mechanism. *Nature* **348**, 239–242.

ARTALEJO, C. R., DAHMER, M. K., PERLMAN, R. L. & FOX, A. P. (1991a). Two types of Ca^{2+} currents are found in bovine chromaffin cells: facilitation is due to the recruitment of one type. *Journal of Physiology* **432**, 681–707.

ARTALEJO, C. R., LÓPEZ, M. G., CASTILLO, C. F., MORO, M. A. & GARCÍA, A. G. (1988). L-type calcium channels and adrenomedullary secretion. In *The Calcium Channel: Structure, Function and Implications*, ed. MORAD, M., NAYLER, W., KAZDA, S. & SCHRAMM, M., pp. 347–362. Springer-Verlag, Berlin.

ARTALEJO, C. R., MOGUL, D. J., PERLMAN, R. L. & FOX, A. P. (1991b). Three types of bovine chromaffin cell Ca^{2+} channels: facilitation increases the opening probability of a 27 pS channel. *Journal of Physiology* **444**, 213–240.

ARTALEJO, C. R., PERLMAN, R. L. & FOX, A. P. (1992a). ω-Conotoxin GVIA blocks a Ca current in bovine chromaffin cells that is not of the 'classic' N-type. *Neuron* **8**, 85–95.

ARTALEJO, C. R., ROSSIE, S., PERLMAN, R. L. & FOX, A. P. (1992b). Voltage-dependent phosphorylation may recruit Ca^{2+} current facilitation in chromaffin cells. *Nature* **358**, 63–66.

BALLESTA, J. J., PALMERO, M., HIDALGO, M. J., GUTIERREZ, L. M., REIG, J. A., VINIEGRA, S. & GARCÍA, A. G. (1989). Separate binding and functional sites for ω-conotoxin and nitrendipine suggest two types of calcium channels in bovine chromaffin cells. *Journal of Neurochemistry* **53**, 1050–1056.

BOSSU, J.-L., DE WAARD, M. & FELTZ, A. (1991a). Inactivation characteristics reveal two calcium currents in adult bovine chromaffin cells. *Journal of Physiology* **437**, 603–620.

BOSSU, J.-L., DE WAARD, M. & FELTZ, A. (1991b). Two types of calcium channels are expressed in adult bovine chromaffin cells. *Journal of Physiology* **437**, 621–634.

CARBONE, E. & LUX, H. D. (1987). Kinetics and selectivity of a low-voltage-activated calcium current in chick and rat sensory neurones. *Journal of Physiology* **386**, 547–570.

CARBONE, E., SHER, E. & CLEMENTI, F. (1990). Ca currents in human neuroblastoma IMR32 cells: kinetics, permeability and pharmacology. *Pflügers Archiv* **416**, 170–179.

CEÑA, V., NICOLAS, G. P., SÁNCHEZ-GARCÍA, P., KIRPEKAR, S. M. & GARCÍA, A. G. (1983). Pharmacological dissection of receptor-associated and voltage-sensitive ionic channels involved in catecholamine release. *Neuroscience* **10**, 1455–1462.

CEÑA, V., STUTZIN, A. & ROJAS, E. (1989). Effects of calcium and Bay K 8644 on calcium currents in adrenal medullary chromaffin cells. *Journal of Membrane Biology* **112**, 255–265.

CHOW, R. H., VON RUDEN, L. & NEHER, E. (1992). Delay in vesicle fusion revealed by electrochemical monitoring of single events in adrenal chromaffin cells. *Nature* **356**, 60–63.

COHEN, C. J. & MCCARTHY, R. T. (1987). Nimodipine block of calcium channels in rat anterior pituitary cells. *Journal of Physiology* **387**, 195–225.

DOUGLAS, W. W. & POISNER, A. M. (1965). Preferential release of adrenaline from the adrenal medulla by muscarine and pilocarpine. *Nature* **208**, 1102–1103.

ELMSLIE, K. S., ZHOU, W. & JONES, S. W. (1990). LHRH and GTP-γ-S modify calcium current activation in bullfrog sympathetic neurons. *Neuron* **5**, 75–80.

FENWICK, E. M., MARTY, A. & NEHER, E. (1982). Sodium and calcium channels in bovine chromaffin cells. *Journal of Physiology* **331**, 599–635.

GANDÍA, L., GARCÍA, A. G. & MORAD, M. (1993). ATP modulation of calcium channels in chromaffin cells. *Journal of Physiology* **470**, 55–72.

GANDÍA, L., LÓPEZ, M. G., FONTERÍZ, R. I., ARTALEJO, C. R. & GARCÍA, A. G. (1987). Relative sensitivities of chromaffin cell calcium channels to organic and inorganic calcium antagonists. *Neuroscience Letters* **77**, 333–338.

GANDÍA, L., MICHELENA, P., DE PASCUAL, R., LÓPEZ, M. G. & GARCÍA, A. G. (1990). Different sensitivities to dihydropyridines of catecholamine release from cat and ox adrenals. *NeuroReport* 1, 119–122.

GARCÍA, A. G., SALA, F., REIG, J. A., VINIEGRA, S., FRIAS, J., FONTERÍZ, R. & GANDÍA, L. (1984). Dihydropyridine Bay-K-8644 activates chromaffin cell calcium channels. *Nature* 308, 69–71.

GRASSI, F. & LUX, H. D. (1989). Voltage-dependent GABA-induced modulation of calcium currents in chick sensory neurons. *Neuroscience Letters* 105, 113–119.

HAMILL, O. P., MARTY, A., NEHER, R., SAKMANN, B. & SIGWORTH, F. J. (1981). Improved patch-clamp techniques for high-resolution current recording from cells and cell-free membrane patches. *Pflügers Archiv* 391, 85–100.

HANS, M., ILLES, P. & TAKEDA, K. (1990). The blocking effects of ω-conotoxin on Ca current in bovine chromaffin cells. *Neuroscience Letters* 114, 63–68.

HIRNING, L. D., FOX, A. P., McCLESKEY, E. W., OLIVERA, B. M., THAYER, S. A., MILLER, R. J. & TSIEN, R. W. (1988). Dominant role of N-type Ca²⁺ channels in evoked release of norepinephrine from sympathetic neurons. *Science* 239, 57–61.

HOSHI, T., ROTHLEIN, J. & SMITH, S. J. (1984). Facilitation of Ca²⁺ channel currents in bovine adrenal chromaffin cells. *Proceedings of the National Academy of Sciences of the USA* 81, 5871–5875.

HOSHI, T. & SMITH, S. J. (1987). Large depolarization induces long openings of voltage-dependent calcium channels in adrenal chromaffin cells. *Journal of Neuroscience* 7, 571–580.

IKEDA, S. R. (1991). Double-pulse calcium current facilitation in adult rat sympathetic neurones. *Journal of Physiology* 439, 181–214.

KASAI, H. & NEHER, E. (1992). Dihydropyridine-sensitive and ω-conotoxin-sensitive calcium channels in a mammalian neuroblastoma–glioma cell line. *Journal of Physiology* 448, 166–188.

LADONA, M. G., AUNIS, D., GANDÍA, L. & GARCÍA, A. G. (1987). Dihydropyridine modulation of the chromaffin cell secretory response. *Journal of Neurochemistry* 48, 483–490.

LÓPEZ, M. G., SHUKLA, R., GARCÍA, A. G. & WAKADE, A. R. (1992). A dihydropyridine-resistant component in the rat adrenal secretory response to splanchnic nerve stimulation. *Journal of Neurochemistry* 58, 2139–2144.

MARCHETTI, C., CARBONE, E. & LUX, H. D. (1986). Effects of dopamine and noradrenaline on Ca channels of cultured sensory and sympathetic neurons of chick. *Pflügers Archiv* 406, 104–111.

MINTZ, I. M., ADAMS, M. E. & BEAN, B. P. (1992). P-type calcium channels in rat central and peripheral neurons. *Neuron* 9, 85–95.

PLUMMER, M. R., LOGOTHETIS, D. E. & HESS, P. (1989). Elementary properties and pharmacological sensitivities of calcium channels in mammalian peripheral neurons. *Neuron* 2, 1453–1463.

POLLO, A., LOVALLO, M., BIANCARDI, E., SHER, E., SOCCI, C. & CARBONE, E. (1993). Sensitivity to dihydropyridines, ω-conotoxin and noradrenaline reveals multiple high-voltage-activated Ca²⁺ channels in rat insulinoma and human pancreatic β-cells. *Pflügers Archiv* 423, 462–471.

POLLO, A., LOVALLO, M., SHER, E. & CARBONE, E. (1992). Voltage-dependent noradrenergic modulation of ω-conotoxin-sensitive Ca²⁺ channels in human neuroblastoma IMR32 cells. *Pflügers Archiv* 422, 75–83.

REGAN, L. J., SAH, D. W. Y. & BEAN, B. P. (1991). Ca²⁺ channels in rat central and peripheral neurons: high-threshold current resistant to dihydropyridine blockers and ω-conotoxin. *Neuron* 6, 269–280.

SHER, E., PANDIELLA, A. & CLEMENTI, F. (1988). ω-Conotoxin binding and effects on calcium channel function in human neuroblastoma and rat pheochromocytoma cell lines. *FEBS Letters* 235, 178–182.

SWANDULLA, D. & ARMSTRONG, C. M. (1988). Fast deactivating calcium channels in chick sensory neurons. *Journal of General Physiology* 92, 197–218.

SWANDULLA, D., CARBONE, E. & LUX, H. D. (1991). Do calcium channel classifications account for neuronal calcium channel diversity? *Trends in Neurosciences* 14, 46–51.

TERBUSH, D. R. & HOLZ, R. W. (1992). Barium and calcium stimulate secretion from digitonin-permeabilized bovine adrenal chromaffin cells by similar pathways. *Journal of Neurochemistry* 58, 680–687.